

Thermodynamics of Liquid Mixtures of Xenon with Alkanes: (Xenon + Ethane) and (Xenon + Propane)

Eduardo J. M. Filipe,* Edmundo J. S. Gomes de Azevedo, Luís F. G. Martins,†
Virgílio A. M. Soares,‡ and Jorge C. G. Calado

Centro de Química Estrutural, Instituto Superior Técnico, 1049-001 Lisboa, Portugal

Clare McCabe§ and George Jackson

Imperial College of Science Technology and Medicine, Prince Consort Road London SW7 2BY, UK

Received: July 14, 1999; In Final Form: November 11, 1999

Total vapor pressures for liquid mixtures of xenon + ethane at 161.40 and 182.34 K and of xenon + propane at 161.40, 182.34, and 195.49 K have been measured. Both systems show negative deviations from Raoult's law at all temperatures. The corresponding excess molar Gibbs energies (G_m^E) have been calculated from the vapor pressure results. Liquid molar volumes have also been measured for both mixtures at 161.40 K, leading to calculated excess molar volumes (V_m^E) which are negative in all cases. Additionally, the excess molar enthalpies (H_m^E) for the xenon + ethane system have been determined directly using a batch calorimeter and found to be negative. Xenon + ethane is thus the simplest system which exhibits negative values for all three major excess molar functions. The results were interpreted using the statistical associating fluid theory for potentials of variable attractive range (SAFT-VR). The theory is able to predict the phase behavior of both systems in close agreement with the experimental results. It was found that the xenon + *n*-alkane mixtures obey Lorentz–Berthelot combining rules, so that no unlike interaction parameters are fitted to experimental mixture data. The theory is therefore totally predictive. It was also found that the parameters calculated for xenon using this model lie within the average values of the parameters obtained for the *n*-alkanes. This implies that, in contrast with the anomalous behavior of methane, xenon can be treated as the first member of the *n*-alkane family. Furthermore, the xenon + *n*-alkane mixtures can be thought as a particular case of mixtures of *n*-alkanes.

1. Introduction

Mixtures of simple molecules still play an important role in the testing and development of statistical theories for the liquid state. In this instance, the adjective “simple” usually means a spherical or quasispherical shape (so that the interaction between molecules can be approximated by a spherically symmetric potential) and negligible quantum effects; pairwise additivity of the intermolecular potential is also taken for granted. This commonly leads to small, positive values of the excess molar Gibbs energy, G_m^E , and negative values of the excess molar volume, V_m^E . Orders of magnitude of the values of these properties for the equimolar mixture are $G_m^E/RT = 0.1$ and $V_m^E/N_A\sigma^3 = -0.01$, where R is the gas constant, N_A Avogadro's number, and σ the molecular diameter. Whereas G_m^E is usually a symmetric function of the composition, V_m^E is often asymmetric, with the minimum shifted toward the more volatile component. The overall phase diagram is of type I (in the Scott–van Konynenburg classification¹).

The molecular behavior of mixtures is determined by the differences in the intermolecular potentials. It has been known

since the time of van der Waals that the crucial parameters are the size and energy ratios for the various molecular pairs. Differences in the size and energy between components, measured by the ratios σ_{11}/σ_{22} and $\epsilon_{11}/\epsilon_{22}$, obviously matter; even more important are the ratios involving the hetero-interaction, for instance σ_{11}/σ_{12} and $\epsilon_{11}/\epsilon_{12}$. Whereas the molecular diameters usually follow Lorentz's rule (the arithmetic mean holding for the cross-interaction, σ_{12}), the energy depth of the potential, ϵ_{12} , deviates a few percent from the geometric mean (also known as Berthelot's rule). If there is a strong attraction between the components, ϵ_{12} is bigger than the geometric mean and σ_{12} is smaller than the arithmetic mean. Already in the 1970s, Monte Carlo simulations had shown² that even for Lorentz–Berthelot binary mixtures, all three major excess functions (G_m^E , H_m^E , and V_m^E) can be negative for particular values of the parameters. In general, G_m^E becomes more positive with increasing values of $\epsilon_{11}/\epsilon_{12}$; for molecules with the same value of ϵ , G_m^E becomes more negative with increasing values of the σ_{11}/σ_{12} ratio. Equivalent correlations were found for the excess molar enthalpy and excess molar volume.²

The first case of a mixture whose experimental values for G_m^E , H_m^E , and V_m^E were all found to be negative was that of xenon + ethane. This special affinity of xenon for the ethane molecule was a surprise, indeed an anomaly among the behavior of simple mixtures. However, a closer examination of the data showed that the results followed the trend predicted by the

† Present address: Departamento de Química, Universidade da Madeira, Caminho da Penteada, 9000 Funchal, Portugal.

‡ Present address: Centro de Ciência e Tecnologia de Materiais, Faculdade de Ciências da Universidade de Lisboa, Campo Grande, Edifício C1, Piso 1, 1700 Lisboa, Portugal.

§ Present address: Department of Chemical Engineering, University of Tennessee, Knoxville, TN 37996.

simulations. Assuming a Lorentz–Berthelot behavior for the mixture and using, as a trial, the molecular parameters for xenon and ethane calculated with the Lennard–Jones one-center model,³ it can be shown that the correlations of Singer and Singer² predict negative values of all excess functions for this system.⁴ Some preliminary results for the xenon + ethane system have been published,⁵ as well as a thorough investigation of its liquid–vapor equilibrium.⁶ This, in turn, led to a systematic investigation of mixtures of xenon with the light *n*-alkanes (linear, branched, and cyclic).

A major development in our understanding of the interaction between xenon and the alkanes was the emergence, in the late 1980s, of the statistical associating fluid theory (SAFT). It has become one of the most powerful predictive tools in the description of phase equilibria for pure fluids and a variety of mixtures. A recent extension of the original approach, SAFT-VR, deals with potentials of variable attractive range, such as the square-well potential. It is this latter version which has been used in this work.

Here we present, for the first time, the vapor–liquid equilibrium and liquid density data in the low-temperature region for the xenon + ethane and xenon + propane systems, as well as the heats of mixing for the former. The molecules are treated as chains of tangentially bonded hard-core segments and the results are discussed and interpreted on the basis of SAFT-VR.

2. Experimental Section

The vapor pressure and density measurements were performed in the same apparatus and carried out isothermally using a triple-point cryostat. Suitable cryogenic substances for the desired temperature range were xenon (triple-point temperature, $T_t = 161.40$ K), nitrous oxide ($T_t = 182.34$ K), and ammonia ($T_t = 195.49$ K). (Temperatures refer to the ITS-90.) The mixtures were prepared condensing known amounts of each component into the pycnometer, with the amount of substance of each component calculated from pVT measurements. The techniques used to measure the saturation vapor pressures and orthobaric densities have already been described in detail elsewhere.⁵ All pressures were measured with a quartz-spiral gauge (Texas Instruments, model 145) which had been calibrated against mercury manometers. The pycnometer used for the density determinations was calibrated with liquid ethane at 161.40 K on the basis of the experimental data of Haynes and Hiza.⁷

The heats of mixing were measured in a batch low-temperature calorimeter described by Lewis and Staveley.⁸ To avoid solidification in the capillary stems, we worked at a slightly higher temperature ($T = 163$ K) than that of the triple point of xenon. The temperature was measured with a copper resistance thermometer previously calibrated by vapor pressure measurements on pure ethane at saturation, using the data of Goodwin.⁹ These measurements revealed that the mixing process is exothermic for this system. Therefore, contrarily to the usual practice, there was no need to supply energy to the system to compensate for the heat of mixing. To calibrate the chart recorder deflection against the heat evolved by the mixing process, a series of four to six heat capacity calibrations were made immediately after the mixing experiment was over. Short heat bursts (10–20 s each) were then supplied to the equilibrium cell, allowing the drift to become linear after each burst.

The gases used in this work (mixture components and cryostat materials) were xenon, ethane, ammonia, nitrous oxide (all from

TABLE 1: Total Vapor Pressure and Excess Molar Gibbs Energy of Xenon + Ethane at 161.40 and 182.34 K^a

<i>x</i>	<i>y</i>	<i>p</i> /kPa	<i>R_p</i> /kPa	<i>G_m^E</i> /J mol ⁻¹
161.40 K				
0	0	23.67	0	0
0.21662	0.46872	35.08	-0.015	-17.53
0.25997	0.52999	37.45	-0.011	-20.44
0.38197	0.67028	44.40	+0.060	-25.40
0.51521	0.78210	52.17	-0.030	-29.00
0.56822	0.81813	55.39	-0.022	-28.18
0.63742	0.85905	59.59	-0.045	-26.43
0.71574	0.89871	64.51	+0.078	-20.45
0.80613	0.93671	69.94	-0.014	-15.78
1	1	81.67	0	0
182.34 K				
0	0	89.90	0	0
0.21615	0.41070	120.41	-0.068	-19.71
0.28699	0.50737	131.12	+0.037	-22.87
0.35017	0.58186	140.80	+0.066	-25.16
0.40331	0.63728	148.99	-0.0003	-26.99
0.50029	0.72509	164.35	+0.004	-27.93
0.54279	0.75870	171.16	-0.030	-27.94
0.60047	0.80045	180.51	-0.059	-27.21
0.71212	0.87024	199.02	-0.004	-23.06
0.81987	0.92614	217.21	+0.079	-16.24
1	1	247.79	0	0

^a R_p are the pressure residuals defined as $R_p = p_{\text{exp}} - p_{\text{calc}}$.

Air Liquide, with stated purities of 99.995%, 99.9%, 99.9%, and 99.99%, respectively), and propane (from Matheson, with a nominal purity of 99.9%). They were all further purified by fractionation in a low-temperature column. The final purity of the samples was checked through the constancy of the triple-point pressure during melting or through their vapor pressures at fixed temperatures. The triple-point pressure of xenon was found to be 81.669 kPa (to be compared with 81.674 ± 0.011 kPa¹⁰); those for the cryostatic fluids also compare favorably with the recommended literature values, 6.093 kPa for ammonia (6.080 ± 0.003 kPa)¹⁰ and 87.815 kPa for nitrous oxide (87.865 ± 0.012 kPa).¹⁰ The triple-point pressures of ethane and propane are too low (1.13 Pa and 1.69×10^{-4} Pa, respectively) to be measured with sufficient accuracy in our apparatus. However, the vapor pressures of these two components at the working temperatures agree, within experimental error, with tabulated values.

The nonideality of the vapor phase was taken into account in the calculations of the phase compositions. Since the pressures never rise above 0.5 MPa, the virial equation of state can be truncated after the second term. Values of the second virial coefficient, B , for xenon were taken from Brewer,¹¹ whereas for ethane the source was Goodwin.⁹ The compilation of Dymond and Smith¹² provided the values of B for ethane and propane at room temperature. Problems arise at very low temperatures for which there are no measured values; a normal procedure is then to use the correlation of Leland.¹³ The cross virial coefficients were taken from ref 14 in the case of the xenon + ethane system. For the xenon + propane mixtures they were estimated using a corresponding states method¹⁵ ($B_{12} = -617$ cm³ mol⁻¹ at 182.34 K, $B_{12} = -534$ cm³ mol⁻¹ at 195.49 K, $B_{12} = -225$ cm³ mol⁻¹ at 298.15 K).

3. Results

Xenon + Ethane System. The total vapor pressures p for xenon + ethane liquid mixtures at 161.40 and 182.34 K are recorded in Table 1 and plotted in Figure 1. The vapor compositions were evaluated using Barker's method¹⁶ which minimizes the pressure residuals $R_p = p - p_{\text{calc}}$. The G_m^E values

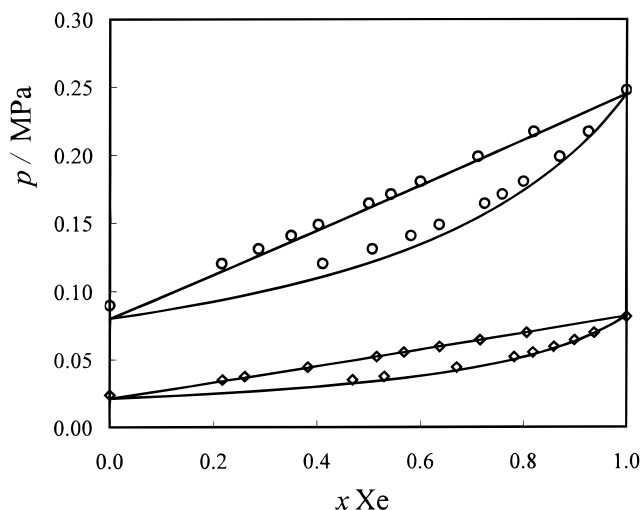


Figure 1. Vapor–liquid equilibrium for the xenon + ethane binary mixture compared with the SAFT-VR predictions. The diamonds represent the experimental results at 161.40 K and the circles at 182.34 K. The theoretical predictions are shown by the continuous curves.

were calculated at zero pressure and fitted to a Redlich–Kister equation,

$$G_m^E/RT = x(1-x)[A + B(1-2x) + C(1-2x)^2] \quad (1)$$

where x is the mole fraction of xenon. The fitting parameters A , B , and C together with their standard deviations and G_m^E ($x = 0.5$) at both temperatures are recorded in Table 2 and the G_m^E curve at 161.40 K is shown in Figure 2. As usual in this type of representation, the curve is the Redlich–Kister eq 1 and the points were calculated with experimental vapor pressures.

The orthobaric molar volumes V_m and excess molar volumes V_m^E of the same system at 161.40 K are given in Table 3. Because of the low pressures involved, the V_m^E values were not corrected to zero pressure since the corrections would be well within experimental error. The excess molar volume results were fitted to a Redlich–Kister type equation,

$$V_m^E/\text{cm}^3 \text{ mol}^{-1} = x(1-x)[D + E(1-2x) + F(1-2x)^2] \quad (2)$$

leading to the following adjusted values for the parameters: $D = -0.4592 \pm 0.0199 \text{ cm}^3 \text{ mol}^{-1}$, $E = 0.1045 \pm 0.0393 \text{ cm}^3 \text{ mol}^{-1}$, and $F = 0.3652 \pm 0.0766 \text{ cm}^3 \text{ mol}^{-1}$. The molar volume residuals $R_v = V_m^E - V_m^E$ (eq 2) are also given in Table 3 and the experimental V_m^E results are presented in Figure 3. For the equimolar mixture, V_m^E ($x = 0.5$) = $-0.115 \pm 0.006 \text{ cm}^3 \text{ mol}^{-1}$.

The results of the excess molar enthalpy measurements H_m^E at 163 K are given in Table 4 and plotted in Figure 2. The values of H_m^E were again fitted to a Redlich–Kister equation

$$H_m^E/RT = x(1-x)[G + H(1-2x) + I(1-2x)^2] \quad (3)$$

The fitting parameters are $G = -0.1527 \pm 0.0050$, $H = 0.0670 \pm 0.0163$, and $I = -0.0125 \pm 0.0588$, giving for the equimolar mixture H_m^E ($x = 0.5$) = $-51.7 \pm 1.7 \text{ J mol}^{-1}$.

Xenon + Propane System. Vapor pressures for xenon + propane measured at 161.40, 182.34, and 195.49 K are recorded in Table 5 and plotted in Figure 4. As before, the vapor compositions were evaluated using Barker's method. The G_m^E

parameters and G_m^E ($x = 0.5$) at all temperatures are recorded in Table 2, and the G_m^E curves are shown in Figure 5. At 161.40 K, the mixtures are almost ideal and consequently the values of G_m^E are very low, showing a larger scatter than usual. From the temperature dependence of G_m^E an average value of H_m^E can be estimated from the Gibbs–Helmholtz equation. A standard procedure using the results of G_m^E at 182.34 and 195.49 K yields a value of $H_m^E = 138 \pm 36 \text{ J mol}^{-1}$ for the equimolar mixture. Being a derived quantity, this value of H_m^E has an uncertainty 1 order of magnitude larger than that of G_m^E . Using this figure to estimate G_m^E at 161.40 K, we obtain a value of $G_m^E = -13 \text{ J mol}^{-1}$, which is in close agreement with the experimental value. Unlike the xenon + ethane system which displays negative values for all major excess molar functions, for xenon + propane the estimated excess molar enthalpy is positive.

The molar volume data for the xenon + propane system at 161.40 K are given in Table 2. As in the case of the xenon + ethane system, no pressure corrections were applied to the experimental data. The V_m^E fitting parameters obtained are $D = -1.2300 \pm 0.0265 \text{ cm}^3 \text{ mol}^{-1}$ and $E = 0.6834 \pm 0.0538 \text{ cm}^3 \text{ mol}^{-1}$. The experimental V_m^E results are presented in Figure 3 where, for the equimolar mixture, V_m^E ($x = 0.5$) = $-0.308 \pm 0.007 \text{ cm}^3 \text{ mol}^{-1}$.

4. Discussion

As mentioned before, the most striking feature of the xenon + ethane mixture is the fact that all four excess functions (G_m^E , H_m^E , S_m^E , and V_m^E) are negative, the first time this type of behavior had been experimentally observed in a simple binary mixture. Nunes da Ponte et al. have also performed vapor–liquid equilibrium measurements for this system in the 210–304 K range.⁶ Their results, although of a lower accuracy, compare favorably with those of this work, and when extrapolated to the vapor–liquid critical line confirm xenon + ethane as a mixture of type I, according to the classification of Scott and van Konynenburg.¹ However, their theoretical calculations using the perturbation theory of Gray and Gubbins failed to reproduce the experimental results.⁶

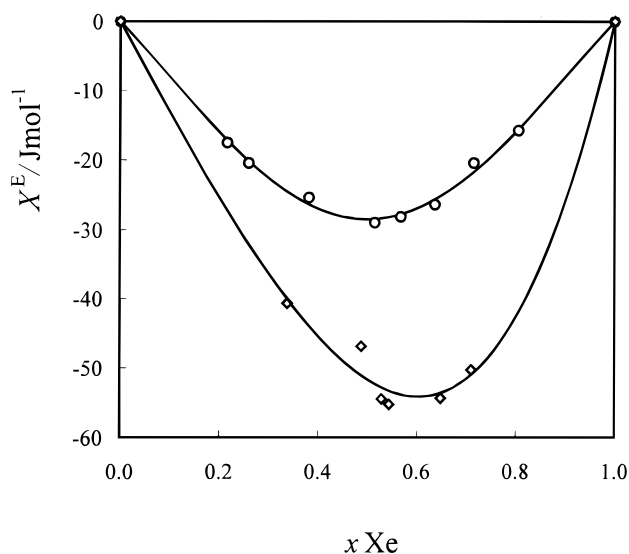
The singular behavior of the xenon + ethane mixtures has been systematically attributed to a strong interaction between the two molecules. Nevertheless, recent measurements of the crossed second virial coefficients for this mixture performed by Ricardo¹⁴ showed no evidence of a specially strong interaction between the xenon and ethane molecules in the dilute gas. This suggests that it is the liquid structure and packing arrangements in the mixture which are responsible for the negative values of the excess functions.

The study of the xenon + propane mixture can be seen as a further step toward the understanding of the nature of the xenon + n -alkane interaction. Once again G_m^E and V_m^E were found to be negative, but H_m^E is estimated to be positive. It should be noted that, mixtures of xenon with butanes also exhibit positive H_m^E (ref 17), suggesting that the xenon + ethane mixture might be the exception to the general rule. (For symmetry reasons, methane should depart even more from the general trends exhibited by the n -alkanes.)

In 1989, Chapman et al. introduced an equation-of-state model for associating fluids^{18,19} the (SAFT). In a simplified version of the original theory, the molecules were modeled as strings of hard spheres with attractive interactions treated at the van der Waals mean-field level. This simplified SAFT-HS approach

TABLE 2: Excess Molar Gibbs Energy of Xenon + Ethane and Xenon + Propane Mixtures at Several Temperatures: Values for the Equimolar Mixture $G_{1/2}^E$ and Coefficients for Eq 1

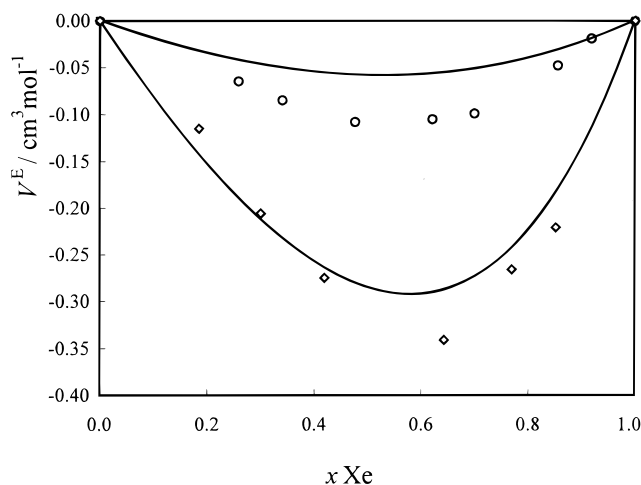
	A	B	C	$G_{1/2}^E/\text{J mol}^{-1}$
xenon + ethane				
161.40 K	-0.0850 ± 0.0023	0.0001 ± 0.0057	0.0288 ± 0.0091	-28.52 ± 0.78
182.34 K	-0.0738 ± 0.0007	-0.0004 ± 0.0021	-0.0030 ± 0.0034	-27.96 ± 0.28
xenon + propane				
161.40 K	-0.0442 ± 0.0150	0.0572 ± 0.0212	0.0514 ± 0.0280	-14.8 ± 5.0
182.34 K	-0.0864 ± 0.0048	-0.0074 ± 0.0080	0.0003 ± 0.0097	-32.75 ± 1.83
195.49 K	-0.1109 ± 0.0099	0.0122 ± 0.0142	0.0269 ± 0.0195	-45.04 ± 4.01

**Figure 2.** Excess molar functions for xenon + ethane. The circles represent the excess molar Gibbs energy at 161.40 K and the diamonds the excess molar enthalpy at 163 K. The lines are the Redlich–Kister expansion (eq 1 and 3).**TABLE 3: Molar Volumes and Excess Molar Volumes of Xenon + Ethane and Xenon + Propane Mixtures at 161.40 K and under Saturation Vapor Pressure^a**

x	$V_m/\text{cm}^3 \text{ mol}^{-1}$	$V_m^E/\text{cm}^3 \text{ mol}^{-1}$	$R_v/\text{cm}^3 \text{ mol}^{-1}$
xenon + ethane			
0	52.548	0	
0.2585	50.325	-0.065	-0.003
0.3401	49.624	-0.085	+0.002
0.4761	48.465	-0.108	+0.005
0.6206	47.262	-0.105	+0.004
0.6995	46.609	-0.099	-0.006
0.8553	45.360	-0.048	-0.005
0.9184	44.861	-0.019	+0.003
1	(44.199)	0	
xenon+propane			
0	67.217	0	
0.1844	62.867	-0.115	-0.005
0.2998	60.124	-0.206	0.005
0.4191	57.316	-0.275	0.002
0.6429	52.112	-0.341	0.014
0.7695	49.279	-0.266	-0.018
0.8515	47.441	-0.221	0.005
1	44.253	0	
0	67.217	0	

^a R_v are the volume residuals defined as $R_v = V_m^E - V_m^E$ (eq 3).

gives a good description of the phase equilibria of strongly associated systems, such as mixtures containing water and hydrogen fluoride.^{20,21} In a recent version of the SAFT approach (SAFT-VR), chain molecules are formed from hard spherical segments with attractive interactions described by a potential of variable range.^{22,23} With this approach, a greatly improved agreement between theoretical predictions of fluid phase

**Figure 3.** Excess molar volumes for xenon + ethane (circles) and xenon + propane (diamonds) at 161.40 K. The theoretical predictions are shown by the continuous curves.**TABLE 4: Excess Molar Enthalpy of Xenon + Ethane at 163 K^a**

x	n_i/mol	Q/J	DU_{corr}	$H_m^E/\text{J mol}^{-1}$
0				0
0.3376	0.04901	-84.4	43.7	-40.7
0.4875	0.07375	-65.9	19.1	-46.9
0.5283	0.06955	-71.7	17.3	-54.5
0.5436	0.06875	-71.5	16.3	-55.3
0.6483	0.07126	-62.4	8.0	-54.4
0.7100	0.06284	-54.0	3.7	-50.3
1				0

^a Q is the electrical energy supplied to the calorimeter (if the mixing was endothermic) to compensate for the enthalpy change on forming an amount of n_i moles of mixture; DU_{corr} is the energy correction due (mostly) to vaporization of the liquid mixture.

equilibria and experimental data is found for systems where the macroscopic behavior is mainly due to dispersion forces.^{24,25}

Before we discuss the results of the SAFT-VR approach for the xenon + n -alkane systems examined in this paper, it is convenient to summarize the main features of the theory; for full details the reader is directed to the original papers.^{22,23}

In the SAFT approach, molecules are modeled as chains of tangentially bonded hard spherical segments of diameter σ . The attractive interactions are described by a square-well potential of variable range λ_{ij} and depth ϵ_{ij} . For the n -alkanes a simple empirical relationship between the number of carbon atoms C in the alkyl chain and the number of spherical segments m in the model chain has been proposed in earlier work:^{20,26} $m = 1 + (C - 1)/3$. Values of $m = 1.33$ and $m = 1.67$ are therefore used for ethane and propane respectively, and a single sphere is naturally used to model the xenon atom.

The Helmholtz free energy A for an n -component mixture of nonassociating chain molecules can be separated into various

TABLE 5: Total Vapor Pressure and Excess Molar Gibbs Energy of Xenon + Propane at 161.40, 182.34, and 195.49 K^a

x	y	p/kPa	R_p/kPa	$G_m^E/\text{J mol}^{-1}$
161.40 K				
0	0	0.946		0
0.1674	0.9411	13.685	-0.252	-1.1
0.2481	0.9635	20.18	+0.219	+3.5
0.3668	0.9784	29.184	+0.141	-5.2
0.4563	0.9849	35.93	-0.239	-16.7
0.5223	0.9885	41.577	-0.00768	-15.5
0.6409	0.9930	51.489	-0.0512	-18.2
0.7054	0.9949	56.989	-0.02265	-16.8
0.7955	0.9969	64.665	+0.03001	-12.6
0.8966	0.9986	73.481	+0.380	-1.0
1	1	81.663		0
182.34 K				
0	0	6.040		0
0.19752	0.89832	48.85	-0.10	-22.56
0.25514	0.92564	62.38	0.22	-24.50
0.39026	0.95906	93.83	-0.23	-33.35
0.55480	0.97891	134.55	0.15	-31.11
0.68712	0.98802	167.73	0.09	-26.68
0.75821	0.99160	185.56	-0.14	-23.80
0.78229	0.99268	191.80	-0.04	-21.45
1	1	247.67		0
195.49 K				
0	0	15.21		0
0.13850	0.79290	65.06	-0.28	-18.26
0.29588	0.91006	125.70	0.38	-32.72
0.43704	0.94982	183.22	0.03	-43.40
0.57944	0.97160	244.57	-0.59	-46.73
0.76412	0.98805	329.59	0.75	-29.28
0.90823	0.99607	394.05	-0.62	-16.26
1	1	436.77		0

^a R_p are the pressure residuals defined as $R_p = p_{\text{exp}} - p_{\text{calc}}$.

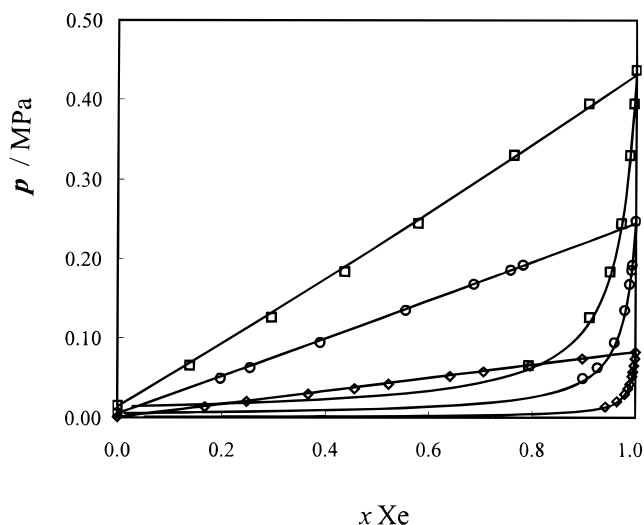


Figure 4. Vapor-liquid equilibrium for the xenon + propane binary mixtures compared with the SAFT-VR predictions. The diamonds represent the experimental results at 161.40 K, the circles at 182.34 K, and the squares at 195.49 K. The theoretical predictions are shown by the continuous curves.

contributions as

$$\frac{A}{NkT} = \frac{A^{\text{IDEAL}}}{NkT} + \frac{A^{\text{MONO.}}}{NkT} + \frac{A^{\text{CHAIN}}}{NkT} \quad (4)$$

where N is the total number of molecules, T the temperature, and k the Boltzmann constant. It should be noted that the

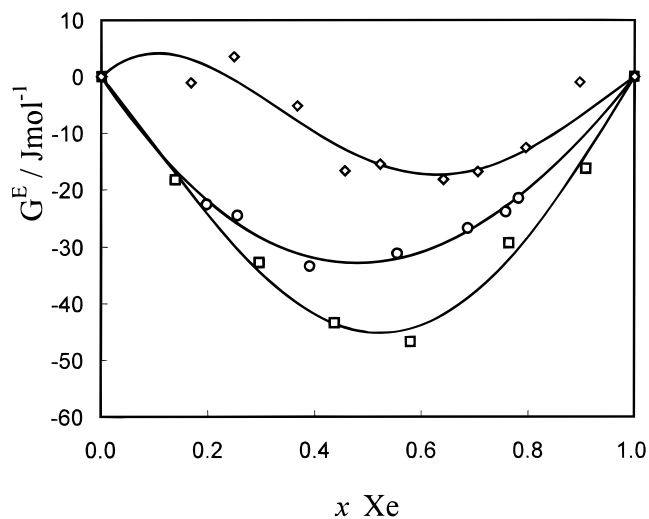


Figure 5. Excess molar Gibbs energy for xenon + propane mixtures at 161.40 K (diamonds), 182.34 K (circles), and 195.49 K (squares). The lines are the Redlich-Kister expansion (eq 1).

association term characteristic of the SAFT approach has not been included because we are dealing with nonassociating systems.

The ideal contribution to the free energy is given by a sum over all species i in the mixture,²⁷

$$\frac{A^{\text{IDEAL}}}{NkT} = \left(\sum_{i=1}^n x_i \ln \rho_i \Lambda_i^3 \right) - 1 \quad (5)$$

where $x_i = N_i/N$ is the mole fraction, $\rho_i = N_i/V$ the number density, N_i the number of molecules, V the volume of the system, and Λ_i the thermal de Broglie wavelength of species i .

We can express the monomer Helmholtz free energy in terms of the free energy *per monomer* a^M ,

$$\frac{A^{\text{MONO}}}{NkT} = \left(\sum_{i=1}^n x_i m_i \right) a^M \quad (6)$$

where m_i is the number of spherical segments of chain i and N_s is the total number of segments. Using the Barker and Henderson²⁸ perturbation theory for mixtures with a hard-sphere reference system, the monomer free energy per segment is obtained from the expansion

$$a^M = a^{\text{HS}} + \beta a_1 + \beta^2 a_2 \quad (7)$$

where $\beta = 1/kT$ and each term is now for a mixture of square-well spherical segments. The expression of Boublik²⁹ and Mansoori et al.³⁰ for a multicomponent mixture of hard spheres is used for the reference hard-sphere term,

$$a^{\text{HS}} = \frac{6}{\pi \rho_s} \left[\left(\frac{\zeta_2^3}{\zeta_3^2} \right) \ln(1 - \zeta_3) + \frac{3\zeta_1 \zeta_2}{(1 - \zeta_3)} + \frac{\zeta_2^3}{\zeta_3(1 - \zeta_3)^2} \right] \quad (8)$$

where $\rho_s = N_s/V$ is the total number density of spherical segments and ζ_i are the reduced densities.

The mean attractive energy, a_1 , is obtained from the sum of the partial terms corresponding to each type of pair interaction, which are written in terms of the contact values of the radial distribution function $g_{ij}^{\text{HS}}(\sigma_{ij}; \zeta_3^{\text{eff}})$ using the mean value theorem,²²

$$a_1 = \sum_{i=1}^n \sum_{j=1}^n x_{s,i} x_{s,j} a_1^{ij}$$

$$a_1^{ij} = -\rho_s \alpha_{ij}^{\text{vdw}} g_{ij}^{\text{HS}}(\sigma_{ij}; \zeta_3^{\text{eff}}) \quad (9)$$

where

$$\alpha_{ij}^{\text{vdw}} = \frac{2}{3} \pi \epsilon_{ij} \sigma_{ij}^3 (\lambda_{ij}^3 - 1) \quad (10)$$

is the van der Waals attractive constant for the i - j square-well interaction, and $g_{ij}^{\text{HS}}(\sigma_{ij}; \zeta_3^{\text{eff}})$ is the radial distribution function for a mixture of hard spheres, evaluated at ζ_3^{eff} , an effective packing fraction.^{22,23} In the evaluation of the perturbation terms, we have used the van der Waals one (VDW-1) fluid approximation (see ref 23 for full details), hence $g_{ij}^{\text{HS}}(\sigma_{ij}; \zeta_3^{\text{eff}})$ in eq 9 is approximated by the radial distribution function for a single fluid giving,

$$a_1^{ij} = -\rho_s \alpha_{ij}^{\text{vdw}} g_0^{\text{HS}}(\sigma_x; \zeta_x^{\text{eff}}) \quad (11)$$

where $g_0^{\text{HS}}(\sigma_x; \zeta_x^{\text{eff}})$ is obtained from the Carnahan and Starling equation of state.³¹ The effective packing fraction ζ_x^{eff} is obtained from the corresponding packing fraction of the fluid ζ_x using,

$$\zeta_x^{\text{eff}}(\zeta_x; \lambda_{ij}) = c_1(\lambda_{ij})\zeta_x + c_2(\lambda_{ij})\zeta_x^2 + c_3(\lambda_{ij})\zeta_x^3 \quad (12)$$

Coefficients c_1 , c_2 , and c_3 are given in ref 22. It should be noted that this corresponds to the MX1b mixing rule of reference.²³

The first fluctuation term a_2 is written in terms of a_1 within the local compressibility approximation,²⁸

$$a_2 = \sum_{i=1}^n \sum_{j=1}^n x_{s,i} x_{s,j} \frac{1}{2} K^{\text{HS}} \epsilon_{ij} \rho_s \frac{\partial a_1^{ij}}{\partial \rho_s} \quad (13)$$

where K^{HS} is the hard-sphere isothermal compressibility of Percus–Yevick.³²

Finally the contribution to the free energy due to chain formation is expressed in terms of the contact value of the background correlation function,^{22,23}

$$\frac{A^{\text{CHAIN}}}{NkT} = -\sum_{i=1}^n x_i (m_i - 1) \ln y_{ii}^{\text{SW}}(\sigma_{ii}) \quad (14)$$

where $y_{ii}^{\text{SW}}(\sigma_{ii}) = g_{ii}^{\text{SW}}(\sigma_{ii}) \exp(-\beta \epsilon_{ii})$ which is obtained from the high-temperature expansion of $y_{ii}^{\text{SW}}(\sigma_{ii})$,

$$y_{ii}^{\text{SW}}(\sigma_{ii}) = g_{ii}^{\text{HS}}(\sigma_{ii}) + \beta \epsilon_{ii} g_1(\sigma_{ii}) \quad (15)$$

The term $g_1(\sigma_{ii})$ is obtained from a self-consistent method for the pressure p from the Clausius virial theorem and from the density derivative of the Helmholtz free energy.²² At this point, the reader should be reminded that only the perturbation terms are evaluated within the VDW-1 fluid approximation and therefore $g_{ij}^{\text{HS}}(\sigma_{ii})$ is evaluated in full, using the expression of Boublík.²⁹

Using standard relationships, all other thermodynamic properties can be obtained from the Helmholtz free energy. Phase equilibrium between phases I and II in a mixture requires that the temperature, pressure, and chemical potential of each

TABLE 6: Optimized Square-Well Intermolecular Potential Parameters for Some n -Alkanes and Xenon^a

substance	m	λ	ϵ/k (K)	σ (nm)
methane	1.00	1.444	168.8	0.3670
ethane	1.33	1.449	241.8	0.3788
propane	1.67	1.452	261.9	0.3873
butane	2.00	1.501	256.3	0.3887
pentane	2.33	1.505	265.0	0.3931
hexane	2.67	1.552	250.4	0.3920
heptane	3.00	1.563	251.3	0.3933
octane	3.33	1.574	250.3	0.3945
xenon	1.00	1.478	243.3	0.3849

^a m is the number of spherical segments in the model, λ the range parameter, σ the diameter of each segment, and ϵ/k the well depth.

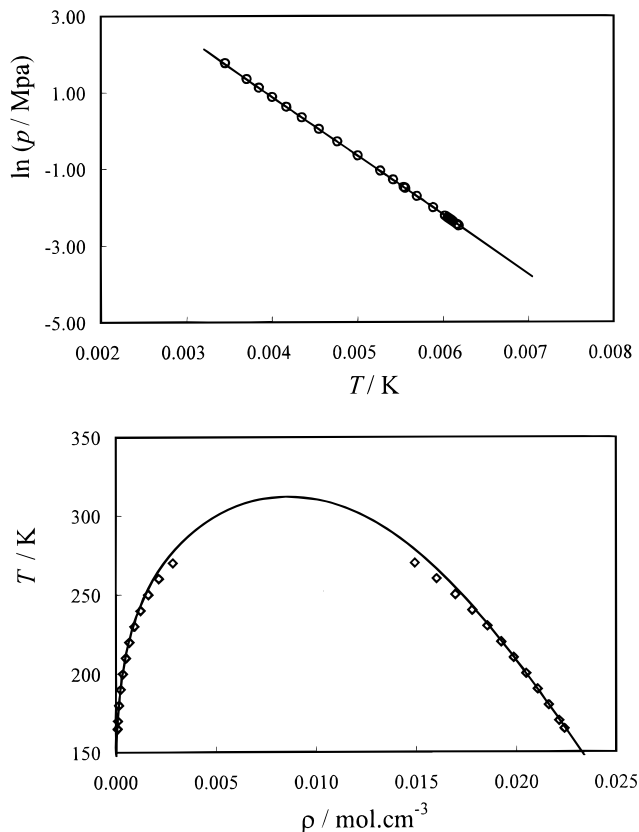


Figure 6. (a) Vapor pressure curve for xenon. (b) Vapor–liquid coexistence densities for xenon. The continuous curves are the SAFT-VR results obtained using parameters fitted simultaneously to vapor pressure and saturated vapor and liquid densities.

component in each phase be equal. These conditions are solved numerically using a simplex method.³⁴

6. Theoretical Results

Before examining the xenon + n -alkane binary mixtures, the parameters of the potential models for the pure components have to be determined. The pure component vapor pressures and saturated liquid densities of each of the pure components are calculated by fitting to experimental data over the entire liquid range. The optimized parameters for xenon are presented in Table 6 along with those of the n -alkanes from previous work.²² In Figure 6, we compare the vapor pressures and coexisting densities for xenon with the experimental data. We show the vapor pressure curve as a Clausius–Clapeyron representation as the excellent agreement between the theoretical prediction and experiment is most clearly illustrated, especially at low temperatures. From the table we note that the n -alkanes, except

for methane and ethane, are described by parameters within an average value of 0.3915 ± 0.0042 nm for σ and 255.9 ± 9.1 K for ϵ/k . It is surprising to see that the xenon parameters are very close to these average values. In other words, according to this model, xenon can be represented as a sphere with almost the same diameter and potential, as those suited to describe the n -alkanes.

The study of phase equilibria in mixtures also requires the determination of a number of unlike parameters, which are obtained from those of the pure components. Lorentz–Berthelot combining rules are used to determine the unlike size and energy parameters²⁹

$$\sigma_{ij} = \frac{\sigma_{ii} + \sigma_{jj}}{2} \quad (16)$$

$$\epsilon_{ij} = \sqrt{\epsilon_{ii}\epsilon_{jj}} \quad (17)$$

and the unlike range parameter is determined from the arithmetic mean,

$$\lambda_{ij} = \frac{\sigma_{ii}\lambda_{ii} + \sigma_{jj}\lambda_{jj}}{\sigma_{ii} + \sigma_{jj}} \quad (18)$$

The SAFT-VR prediction for the constant temperature p,x slices of the xenon + ethane binary mixture are presented alongside the experimental data in Figure 1. The theory is able to accurately reproduce the experimental data and the negative deviation from Raoult's law. In Figure 4, we present the theoretical prediction for the xenon + propane system compared with the experimental data of Table 5. The SAFT-VR approach again describes the gas–liquid coexistence envelopes in excellent agreement with the experimental data. Finally, in Figure 3 we compare the experimental excess molar volumes for both systems with the SAFT-VR prediction. As can be seen the theory is able to accurately predict both the sign and order of magnitude of the experimental data. It should be emphasized that no experimental data for the mixtures was used in the calculations; that is, the results are pure predictions. It can be concluded that the basic physical requirements (relative size, interaction, and shape) are adequately taken into account. It should also be stressed that xenon's VLE properties are well described by treating it as a sphere with similar characteristics to those used to describe the n -alkanes, implying that xenon behaves as an n -alkane. Ultimately, this also implies that mixtures of xenon + n -alkane can be thought as a particular case of mixtures of n -alkanes. Indeed, it is found that mixtures of n -alkanes, except for those involving methane, do deviate negatively from Raoult's law and exhibit negative excess Gibbs energies and negative excess volumes.³³ Taking into account the van der Waals radii, it is interesting to note that the diameter of the xenon atom is comparable to the n -alkane molecules cross diameter, as suggested by the SAFT-VR model. The similarities between xenon and the n -alkanes extend to other fields such as anesthesia, and a paper on this subject will be published shortly.

Acknowledgment. L.F.G.M. thanks the Foundation for Science and Technology (FCT) for the award of a grant (CIÊNCIA/BD/2720/93-RM). E.J.M.F. gratefully acknowledges a grant through the European Science Exchange Program between the Lisbon Academy of Sciences (ACL) and the Royal Society.

References and Notes

- (1) van Konynenburg, P. H.; Scott, R. L. *Philos. Trans. R. Soc. London A* **1980**, 298, 495.
- (2) Singer, J. V. L.; Singer, K. *Mol. Phys.* **1972**, 25, 251.
- (3) Bohn, M.; Lustig, R.; Fisher, J. *Fluid Phase Equil.* **1986**, 25, 251.
- (4) Filipe, E. J. M. Ph.D. Thesis, Instituto Superior Técnico, Lisboa, 1993.
- (5) Calado, J. C. G.; Gomes de Azevedo, E. J. S.; Soares, V. A. M. *Chem. Eng. Commun.* **1980**, 5, 149.
- (6) Nunes da Ponte, M.; Chokappa, D.; Calado, J. C. G.; Clancy, P.; Streett, W. B. *J. Phys. Chem.* **1985**, 89, 2746.
- (7) Haynes, W. M.; Hiza, M. J. *J. Chem. Thermodyn.* **1977**, 9, 179.
- (8) Lewis, K. L.; Staveley, L. A. K. *J. Chem. Thermodyn.* **1975**, 7, 855.
- (9) Goodwin, R. D.; Roder, H. M.; Straty, G. C. *NBS Technical Report 684*; National Bureau of Standards: Boulder, 1976.
- (10) Staveley, L. A. K.; Lobo, L. Q.; Calado, J. C. G. *Cryogenics* **1981**, 21, 131.
- (11) Brewer, J. *Report MRL-2915-C, AFOSR-67-2795*, 1968.
- (12) Dymond, J. B.; Smith, E. B. *The Virial Coefficients of Pure Gases and Mixtures*; Clarendon Press: Oxford, 1980.
- (13) Leland, T. W.; Chappellear, P. S. *Ind. Eng. Chem.* **1968**, 60, 15.
- (14) Aguiar Ricardo, A.; Nunes da Ponte, M. *J. Phys. Chem.* **1996**, 100, 18839.
- (15) Reid, R. C.; Prausnitz, J. M.; Poling, B. E. *The Properties of Gases and Liquids*, 4th ed.; McGraw-Hill Book Co.: Singapore, 1988.
- (16) Barker, J. A. *Aust. J. Chem.* **1953**, 6, 207.
- (17) In preparation.
- (18) Chapman, W. G.; Gubbins, K. E.; Jackson, G.; Radosz, M. *Fluid Phase Equil.* **1989**, 52, 31.
- (19) Chapman, W. G.; Gubbins, K. E.; Jackson, G.; Radosz, M. *Ind. Eng. Chem. Res.* **1990**, 29, 1709.
- (20) Galindo, A.; Whitehead, P. J.; Jackson, G.; Burgess, A. N. *J. Phys. Chem.* **1996**, 100, 6781.
- (21) Galindo, A.; Whitehead, P. J.; Jackson, G.; Burgess, A. N. *J. Phys. Chem.* **1997**, 101, 2082.
- (22) Gil-Villegas, A.; Galindo, A.; Whitehead, P. J.; Mills, S. J.; Jackson, G.; Burgess, A. N. *J. Chem. Phys.* **1997**, 106, 4168.
- (23) Galindo, A.; Davies, L. A.; Gil-Villegas, A.; Jackson, G. *Mol. Phys.* **1998**, 93, 241.
- (24) McCabe, C.; Galindo, A.; Gil-Villegas, A.; Jackson, G. *Int. J. Thermophys.* **1998**, 19, 1511.
- (25) McCabe, C.; Gil-Villegas, A.; Jackson, G. *J. Phys. Chem.* **1998**, 102, 4183.
- (26) Jackson, G.; Gubbins, K. E. *Pure Appl. Chem.* **1989**, 61, 1021.
- (27) Hansen, J. P.; McDonald, I. R. *Theory of Simple Liquids*, 2nd ed.; Academic Press: London, 1986.
- (28) Leonard, P. J.; Henderson, D.; Barker, J. A. *Trans. Faraday Soc.* **1970**, 66, 2439.
- (29) Boublik, T. *J. Chem. Phys.* **1970**, 53, 471.
- (30) Mansoori, G. A.; Carnahan, N. F.; Starling, K. E.; Leland, T. W. *J. Chem. Phys.* **1971**, 54, 1523.
- (31) Carnahan, N. F.; Starling, K. E. *J. Chem. Phys.* **1969**, 51, 635.
- (32) Reed, T. M.; Gubbins, K. E. *Applied Statistical Mechanics*; McGraw-Hill: New York, 1973.
- (33) Rowlinson, J. S.; Swinton, F. L. *Liquids and Liquid Mixtures*, 3rd ed.; Butterworth Scientific: London, 1982.
- (34) Press, W. H.; Teukolsky, S. A.; Vetterling, W. T.; Flannery, B. P. *Numerical Recipes in Fortran*, 1st ed.; Cambridge University Press: Cambridge, 1986.